

# Thermodynamic basis for the optimization of binding-induced biomolecular switches and structure-switching biosensors

Alexis Vallée-Bélisle<sup>a</sup>, Francesco Ricci<sup>a,1</sup>, and Kevin W. Plaxco<sup>a,b,2</sup>

<sup>a</sup>Department of Chemistry and Biochemistry, <sup>b</sup>Interdepartmental Program in Biomolecular Science and Engineering, University of California, Santa Barbara, CA 93106

Edited by David Baker, University of Washington, Seattle, WA, and approved June 24, 2009 (received for review April 12, 2009)

**Binding-induced biomolecular switches are used throughout nature and, increasingly, throughout biotechnology for the detection of chemical moieties and the subsequent transduction of this detection into useful outputs. Here we show that the thermodynamics of these switches are quantitatively described by a simple 3-state population-shift model, in which the equilibrium between a nonbinding, nonsignaling state and the binding-competent, signaling state is shifted toward the latter upon target binding. Because of this, their performance is determined by the tradeoff inherent to their switching thermodynamics; while a switching equilibrium constant favoring the nonbinding, nonsignaling, conformation ensures a larger signal change (more molecules are poised to respond), it also reduces affinity (binding must overcome a more unfavorable conformational free energy). We then derive and employ the relationship between switching thermodynamics and switch signaling to rationally tune the dynamic range and detection limit of a representative structure-switching biosensor, a molecular beacon, over 4 orders of magnitude. These findings demonstrate that the performance of biomolecular switches can be rationally tuned via mutations that alter their switching thermodynamics and suggest a mechanism by which the performance of naturally occurring switches may have evolved.**

allostery | ligand-induced conformational change | pre-existing equilibrium | rational design, sensitivity | riboswitches

**B**inding-induced conformational changes are used in nature and, increasingly, in biotechnology for the detection of chemical moieties and the subsequent transduction of that recognition into useful outputs. Among the many examples offered by nature (1, 2) are the calmodulin proteins, which regulate cellular processes via a calcium-triggered conformational change (3, 4), and the cytokine receptors, which signal through the cell membrane via a hormone-induced conformational change (5, 6) (Fig. 1, *Top*). Other examples include intrinsically disordered proteins, which regulate multiple cellular processes when they fold upon binding to their target ligands (7–9), and riboswitches, which regulate translation via a metabolite-induced conformational change in the mRNA leader sequence (10). Similar structure-switching biomolecules, either naturally occurring (11–14), artificially selected (15–21), or rationally designed examples (21–30), have been used for diagnostic applications (31) in synthetic biology (32, 33) and in situ real time imaging (34). Examples of these include synthetic riboswitches for the control of gene expression (26) and metabolic pathways (33), fluorescent sensors for the detection of intracellular calcium (11) (Fig. 1, *Middle*), and molecular beacons for the detection of specific oligonucleotide sequences (22) (Fig. 1, *Bottom*).

Ligand-induced biomolecular switches are generally thought to function via a 3-state population-shift mechanism (Fig. 1) in which the naturally occurring equilibrium between a nonbinding, nonsignaling state, and the binding-competent signaling state, is shifted toward the latter upon target binding (35–41) [n.b., their

kinetics may be equally simple (14) or significantly more complex (42, 43)]. Because of this, the function of binding-induced switches embodies a tradeoff: While a switching equilibrium constant shifted toward the nonbinding conformation ensures a larger signal change (more molecules are poised to respond), it also reduces affinity (binding must overcome a more unfavorable conformational free energy). This, in turn, implies that, as previously noted, the thermodynamics of switching will affect the switch's dynamic range (28, 37, 44) and detection limit (28, 45). Starting from these qualitative arguments, we derive here a quantitative population-shift model and employ it to: (i) Describe and test the relationship between switch signaling and switching thermodynamics and (ii) rationally optimize the performance of a representative switch. The implications of these findings for the evolution of natural biomolecular switches are also discussed.

## Results

To elucidate the relationship between switching thermodynamics and signaling, we have studied molecular beacons (Fig. 1, *Bottom*), synthetic biomolecular switches developed by Kramer and coworkers (22), and widely used in the diagnosis of genetic and infectious diseases (31, 46, 47). Consisting of a stem-loop DNA modified with a fluorophore/quencher pair, molecular beacons provide an ideal test bed for our studies; their simple, stem-loop structure separates the determinants that define affinity (the loop) from those that define the switching equilibrium (the stem). From the perspective of the population-shift model, the mechanism of molecular beacons relies on the equilibrium between the non-emissive stem-loop conformation (the nonbinding state) and the emissive extended conformation (the binding-competent state) that is shifted to the latter upon hybridization with a complementary oligonucleotide (Fig. 1, *Bottom*).

We have constructed a set of 6 molecular beacons that retain a common loop sequence (and thus maintain a constant intrinsic affinity,  $K_D^{\text{int}}$ , for their target) but differ in their stem sequences (thus modulating the switching equilibrium constant,  $K_S$ ). To determine the switching equilibrium constant of each variant, we used urea denaturation (Fig. 2), a method that has seen widespread use in the determination of folding free energies (48, 49). The unfolding curves of all 6 of our molecular beacons are well-fitted as 2-state unfolding transitions with switching equi-

Author contributions: A.V.-B., F.R., and K.W.P. designed research; A.V.-B. performed research; A.V.-B. and K.W.P. contributed new reagents/analytic tools; A.V.-B., F.R., and K.W.P. analyzed data; and A.V.-B., F.R., and K.W.P. wrote the paper.

The authors declare no conflict of interest.

This article is a PNAS Direct Submission.

<sup>1</sup>Present address: Dipartimento di Scienze e Tecnologie Chimiche, University of Rome, Tor Vergata, Via della Ricerca Scientifica, 00133, Rome, Italy.

<sup>2</sup>To whom correspondence should be addressed. E-mail: kwp@chem.ucsb.edu.

This article contains supporting information online at [www.pnas.org/cgi/content/full/0904005106/DCSupplemental](http://www.pnas.org/cgi/content/full/0904005106/DCSupplemental).







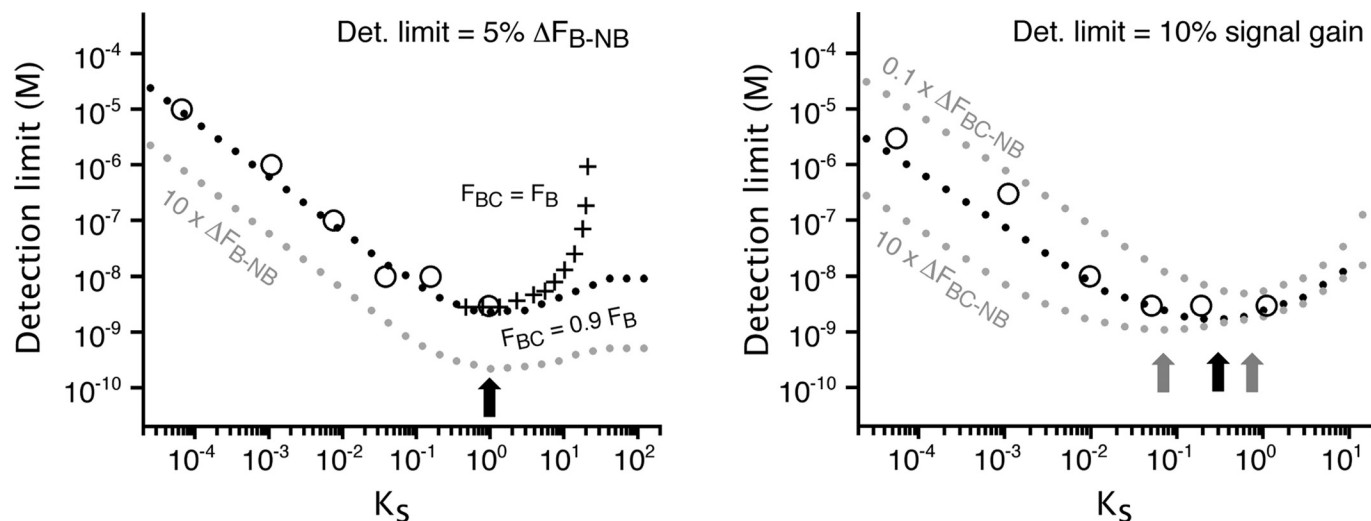


**Fig. 5.** Optimal detection limits are achieved at intermediate values of the switching equilibrium constant,  $K_S$ . Shown are experimentally determined (open circles) or predicted (black dotted lines) detection limits for our molecular beacons as a function of their  $K_S$  when using different detection limit definitions. (Left) When the detection limit is defined as the target concentration that produces an absolute signal,  $\Delta F$ , that is 5% of the maximum possible signal change ( $\Delta F = 0.05\Delta F_{B-NB}$ , which reflects a realistic detection limit for our fluorimeter), the optimal switching equilibrium constant is near unity (arrow). This optimal value is also independent of the relative fluorescence of the bound and nonbinding states (gray dotted line). At still higher values of  $K_S$ , the detection limit becomes poorer, although the magnitude of this effect depends on the difference in the fluorescence of the bound and binding-competent states (compare crosses and dotted line). (Right) If, in contrast, the detection limit is defined as the target concentration that produces a 10% change in relative fluorescence (a realistic detection limit for our fluorimeter), the optimal switching equilibrium constant is near 0.3. Under this definition of detection limit, however, the optimal value of  $K_S$  is obviously sensitive to  $\Delta F_{BC-NB}$ ; the higher this latter value is, the lower the optimal  $K_S$  will be to minimize the population of switches in the binding-competent state that signal in absence of target [i.e., minimize  $F(0)$ ; see Eq. 4]. All simulations were performed using  $F_{BG} = 0.23$  (background fluorescence),  $F_{NB} = 0.04$  (obtained using Fig. 3, Top), and  $K_A^{int} = 6.7 \times 10^7 \text{ M}^{-1}$  (Fig. 3, Bottom).  $\Delta F_{BC-NB}$  was set to  $0.9 \Delta F_{B-NB}$  for all simulations (unless specified), as it is observed experimentally for our molecular beacons (Fig. 4).

such as *mfold*, provide relatively accurate estimates of specific RNA or DNA conformations (52). Similar approaches can be, and indeed, have already been used to tune the switching thermodynamics of protein-based switches. And while the lack of a simple base-pairing code renders the rational optimization of their switching thermodynamics more complex, several approaches to tuning the switching equilibria of proteins have been reported (37). For example, Marvin and Hellinga identified a key residue that controls the switching thermodynamics of the bacterial periplasmic binding protein superfamily simply by comparing the structures of their bound and unbound states (44). Abadou and Desjarlais have stabilized the nonbinding conformation of the N-terminal EF-hand domain of calmodulin—and thus reducing its calcium binding affinity—by replacing partially buried polar residues with hydrophobic residues (53). Springer, Mayo, and colleagues have used computational redesign of hydrophobic cores to specifically stabilize the open “binding-competent” or closed “nonbinding” states of the Mac1 integrin I (54). Lockless and Ranganathan have developed a technique termed statistical coupling analysis that employs evolutionary data to map residues that control conformational switching (55, 56). Finally, we have shown that binding-induced protein folding, which is perhaps a more generic protein-based switching mechanism (7–9, 57), is readily tuned via substitutions distant from the binding interface that stabilize or destabilize the native state (14).

In addition to providing a rational framework to guide the design of optimized structure-switching biosensors, the thermodynamic principles presented here may also improve our understanding of the mechanisms behind the evolution of naturally occurring biomolecular switches. An example of this is provided by the 2 homologous calcium binding EF-hand domains of calmodulin which, despite 75% sequence homology, differ significantly in their calcium affinity (58–60). The apo form of the lower affinity domain adopts a closed,

nonbinding conformation that is stabilized by a well-buried phenylalanine (3, 60). In contrast, in the higher affinity domain, this residue is replaced by the more hydrophilic tyrosine, which is thought to promote a partially open, binding-competent state that, in turn, leads to improved calcium binding (3, 60). The distinct calcium affinities of the 2 domains, in turn, are thought to play an important role in the “wrap around” mechanism by which calmodulin binds many of its polypeptide targets by supporting the sequential attachment of the domains as the calcium concentration increases (4, 60). A second set of examples is provided by the intrinsically disordered proteins, proteins that only fold upon binding to their specific target (7–9). This binding-induced folding-switch mechanism, which has been used in several protein-based biosensors (14, 57), has been proposed as an efficient strategy by which nature reduces the affinity of biomolecules without simultaneously reducing their specificity (8, 61). As our knowledge of the thermodynamics of natural biomolecular switches progresses, it will be interesting to uncover how their switching thermodynamics have evolved to achieve optimal performance *in vivo*.

## Materials and Methods

HPLC-purified molecular beacons modified with a 5'-FAM and a 3'-BHQ-1 and aliquots of the 13-nucleotide target were purchased from Sigma-Genosys (all constructs possess an additional Adenine nucleotide, after the FAM, and Guanine nucleotide, before the BHQ-1). Ultrapure urea was obtained from USB Corporation. All experiments were conducted at pH 7.0 in 50 mM sodium phosphate buffer, 150 mM NaCl, at 45 °C. All fluorescence measurements were obtained using a Cary Eclipse Fluorimeter (Varian) with excitation at 480 ( $\pm 5$ ) nm and acquisition between 514 and 520 nm using either 5 nm (unfolding curves) or 20 nm (binding curves) bandwidths. Urea unfolding curves were obtained using 500 nM of molecular beacon by sequentially increasing (or decreasing for 4GC, 5GC) the urea concentration of a 0 M urea sample (8 M for 4GC, 5GC) with 8 M urea (0 M for 4GC, 5GC) containing the same concentration of molecular beacon. The fluorescence of the open state was set relative to 1.

The switching equilibrium constants of all molecular beacons (stability of the nonbinding state) were obtained by global fitting the unfolding curves with a 2-state folding/unfolding model (48) using the same average  $m$ -value ( $2.4 \text{ kJ mol}^{-1} \text{ M}^{-1}$ ) and same values for the effect of the urea on the fluorescence of the folded ( $0.011 \text{ M}^{-1}$ ) and unfolded-state ( $-0.0087 \text{ M}^{-1}$ ) as obtained for the molecular beacons 5GC and 0GC, respectively. The 5GC molecular beacon is relatively stable to denaturation by 8 M urea (Fig. 2), and thus its free energy was estimated using the *mfold* prediction algorithm (51) (see Fig. S1). Binding curves were obtained using 3 nM molecular beacon by sequentially increasing the target concentration via the addition of small volumes of solutions with increasing concentration of target and the same molecular beacon concentration. All binding curves (Fig. 3, Top) were normalized by setting the bound state fluorescence to the  $F_B$  obtained for 0GC (4.5), and the observed  $K_D$  were obtained using:

$$F([T]) = F(0) + \left( \frac{[T](F_B - F(0))}{[T] + K_D^{\text{obs}}} \right) \quad [5]$$

Simulations (Figs. 4, Right, and 5) were generated using Eq. 3 (absolute signal change) or Eq. 4 (signal gain) by determining the signal change or signal gain produced by the addition of various concentrations of target for each molecular beacon.

**ACKNOWLEDGMENTS.** We thank Prof. Fred Kramer, Prof. Stephen Michnick, and members of our research group for helpful discussions and comments on the manuscript. This work was supported by the National Institutes of Health Grant R01EB007689. A.V.-B. is a Fonds Québécois de la Recherche sur la Nature et les Technologies Fellow.

- Gerstein M, Krebs W (1998) A database of macromolecular motions. *Nucleic Acids Res* 26:4280–4290.
- Goh CS, Milburn D, Gerstein M (2004) Conformational changes associated with protein-protein interactions. *Curr Opin Struct Biol* 14:104–109.
- Swindells MB, Ikura M (1996) Pre-formation of the semi-open conformation by the apo-calmodulin C-terminal domain and implications binding IQ-motifs. *Nat Struct Biol* 3:501–504.
- Chin D, Means AR (2000) Calmodulin: A prototypical calcium sensor. *Trends Cell Biol* 10:322–328.
- Remy I, Wilson IA, Michnick SW (1999) Erythropoietin receptor activation by a ligand-induced conformation change. *Science* 283:990–993.
- Stroud RM, Wells JA (2004) Mechanistic diversity of cytokine receptor signaling across cell membranes. *Sci STKE* 2004:re7.
- Wright PE, Dyson HJ (1999) Intrinsically unstructured proteins: Re-assessing the protein structure-function paradigm. *J Mol Biol* 293:321–331.
- Dunker AK, et al. (2001) Intrinsically disordered protein. *J Mol Graphics Model* 19:26–59.
- Dunker AK, Silman I, Uversky VN, Sussman JL (2008) Function and structure of inherently disordered proteins. *Curr Opin Struct Biol* 18:756–764.
- Roth A, Breaker RR (2009) The structural and functional diversity of metabolite-binding riboswitches. *Annu Rev Biochem* 78:305–334.
- Miyawaki A, et al. (1997) Fluorescent indicators for  $\text{Ca}^{2+}$  based on green fluorescent proteins and calmodulin. *Nature* 388:882–887.
- Marvin JS, et al. (1997) The rational design of allosteric interactions in a monomeric protein and its applications to the construction of biosensors. *Proc Natl Acad Sci USA* 94:4366–4371.
- Benson DE, Conrad DW, de Lorimier RM, Trammell SA, Hellinga HW (2001) Design of bioelectronic interfaces by exploiting hinge-bending motions in proteins. *Science* 293:1641–1644.
- Kohn JE, Plaxco KW (2005) Engineering a signal transduction mechanism for protein-based biosensors. *Proc Natl Acad Sci USA* 102:10841–10845.
- Nutiu R, Li Y (2005) Aptamers with fluorescence-signaling properties. *Methods* 37:16–25.
- Stojanovic MN, de Prada P, Landry DW (2001) Aptamer-based folding fluorescent sensor for cocaine. *J Am Chem Soc* 123:4928–4931.
- Buskirk AR, Liu DR (2005) Creating small-molecule-dependent switches to modulate biological functions. *Chem Biol* 12:151–161.
- Guntas G, Mansell TJ, Kim JR, Ostermeier M (2005) Directed evolution of protein switches and their application to the creation of ligand-binding proteins. *Proc Natl Acad Sci USA* 102:11224–11229.
- Ostermeier M (2005) Engineering allosteric protein switches by domain insertion. *Protein Eng Des Sel* 18:359–364.
- Tang Z, et al. (2008) Aptamer switch probe based on intramolecular displacement. *J Am Chem Soc* 130:11268–11269.
- Wright CM, Heins RA, Ostermeier M (2007) As easy as flipping a switch? *Curr Opin Chem Biol* 11:342–346.
- Tyagi S, Kramer FR (1996) Molecular beacons: Probes that fluoresce upon hybridization. *Nat Biotechnol* 14:303–308.
- Ambroggio XI, Kuhlman B (2006) Design of protein conformational switches. *Curr Opin Struct Biol* 16:525–530.
- Hall B, Hesselberth JR, Ellington AD (2007) Computational selection of nucleic acid biosensors via a slip structure model. *Biosens Bioelectron* 22:1939–1947.
- Sallee NA, Yeh BJ, Lim WA (2007) Engineering modular protein interaction switches by sequence overlap. *J Am Chem Soc* 129:4606–4611.
- Win MN, Smolke CD (2008) Higher-order cellular information processing with synthetic RNA devices. *Science* 322:456–460.
- Strickland D, Moffat K, Sosnick TR (2008) Light-activated DNA binding in a designed allosteric protein. *Proc Natl Acad Sci USA* 105:10709–10714.
- Beisel CL, Bayer TS, Hoff KG, Smolke CD (2008) Model-guided design of ligand-regulated RNAi for programmable control of gene expression. *Mol Syst Biol* 4:224.
- Lee J, et al. (2008) Surface sites for engineering allosteric control in proteins. *Science* 322:438–442.
- Xiao Y, Qu X, Plaxco KW, Heeger AJ (2007) Label-free electrochemical detection of DNA in blood serum via target-induced resolution of an electrode-bound DNA pseudoknot. *J Am Chem Soc* 129:11896–11897.
- Marras SA, Tyagi S, Kramer FR (2006) Real-time assays with molecular beacons and other fluorescent nucleic acid hybridization probes. *Clin Chim Acta* 363:48–60.
- Isaacs FJ, Dwyer DJ, Collins JJ (2006) RNA synthetic biology. *Nat Biotechnol* 24:545–554.
- Keasling JD (2008) Synthetic biology for synthetic chemistry. *ACS Chem Biol* 3:64–76.
- Giepmans BN, Adams SR, Ellisman MH, Tsien RY (2006) The fluorescent toolbox for assessing protein location and function. *Science* 312:217–224.
- Monod J, Wyman J, Changeux JP (1965) On the nature of allosteric transitions: A plausible model. *J Mol Biol* 12:88–118.
- Tsai CJ, Ma B, Nussinov R (1999) Folding and binding cascades: Shifts in energy landscapes. *Proc Natl Acad Sci USA* 96:9970–9972.
- Mizoue LS, Chazin WJ (2002) Engineering and design of ligand-induced conformational change in proteins. *Curr Opin Struct Biol* 12:459–463.
- James LC, Roversi P, Tawfik DS (2003) Antibody multispecificity mediated by conformational diversity. *Science* 299:1362–1367.
- Cui Q, Karplus M (2008) Allosteric and cooperativity revisited. *Protein Sci* 17:1295–1307.
- Okazaki K, Takada S (2008) Dynamic energy landscape view of coupled binding and protein conformational change: Induced-fit versus population-shift mechanisms. *Proc Natl Acad Sci USA* 105:11182–11187.
- Gsponer J, et al. (2008) A coupled equilibrium shift mechanism in calmodulin-mediated signal transduction. *Structure* 16:736–746.
- Weikl TR, von Deuster C (2009) Selected-fit versus induced-fit protein binding: Kinetic differences and mutational analysis. *Proteins* 75:104–110.
- Shoemaker BA, Portman JJ, Wolynes PG (2000) Speeding molecular recognition by using the folding funnel: The fly-casting mechanism. *Proc Natl Acad Sci USA* 97:8868–8873.
- Marvin JS, Hellinga HW (2001) Manipulation of ligand binding affinity by exploitation of conformational coupling. *Nat Struct Biol* 8:795–798.
- Kim JR, Ostermeier M (2006) Modulation of effector affinity by hinge region mutations also modulates switching activity in an engineered allosteric TEM1 beta-lactamase switch. *Arch Biochem Biophys* 446:44–51.
- Wang K, et al. (2009) Molecular engineering of DNA: Molecular beacons. *Angew Chem Int Ed Engl* 48:856–870.
- El-Hajj HH, et al. (2009) Use of sloppy molecular beacon probes for identification of mycobacterial species. *J Clin Microbiol* 47:1190–1198.
- Pace CN (1986) Determination and analysis of urea and guanidine hydrochloride denaturation curves. *Methods Enzymol* 131:266–280.
- Shelton VM, Sosnick TR, Pan T (1999) Applicability of urea in the thermodynamic analysis of secondary and tertiary RNA folding. *Biochemistry* 38:16831–16839.
- Sosnick TR, Krantz BA, Dothager RS, Baxa M (2006) Characterizing the protein folding transition state using psi analysis. *Chem Rev* 106:1862–1876.
- Marras SA, Kramer FR, Tyagi S (2002) Efficiencies of fluorescence resonance energy transfer and contact-mediated quenching in oligonucleotide probes. *Nucleic Acids Res* 30:e122.
- SantaLucia J, Jr (1998) A unified view of polymer, dumbbell, and oligonucleotide DNA nearest-neighbor thermodynamics. *Proc Natl Acad Sci USA* 95:1460–1465.
- Ababou A, Desjarlais JR (2001) Solvation energetics and conformational change in EF-hand proteins. *Protein Sci* 10:301–312.
- Shimaoka M, et al. (2000) Computational design of an integrin I domain stabilized in the open high affinity conformation. *Nat Struct Biol* 7:674–678.
- Lockless SW, Ranganathan R (1999) Evolutionarily conserved pathways of energetic connectivity in protein families. *Science* 286:295–299.
- Hatley ME, Lockless SW, Gibson SK, Gilman AG, Ranganathan R (2003) Allosteric determinants in guanine nucleotide-binding proteins. *Proc Natl Acad Sci USA* 100:14445–14450.
- Oh KJ, Cash KJ, Plaxco KW (2009) Beyond molecular beacons: Optical sensors based on the binding-induced folding of proteins and polypeptides. *Chemistry* 15:2244–2251.
- Minowa O, Yagi K (1984) Calcium binding to tryptic fragments of calmodulin. *J Biochem* 96:1175–1182.
- Linse S, Helmersson A, Forsen S (1991) Calcium binding to calmodulin and its globular domains. *J Biol Chem* 266:8050–8054.
- Bhattacharya S, Bunick CG, Chazin WJ (2004) Target selectivity in EF-hand calcium binding proteins. *Biochim Biophys Acta* 1742:69–79.
- Schulz GE (1979) Nucleotide binding proteins, in *Molecular Mechanism of Biological Recognition*, ed Balaban M (Elsevier/North-Holland Biomedical Press, New York, NY), pp 79–94.